Title
Hydrophobic Inorganic Oxide Pigments via Polymethylhydrosiloxane Grafting: Dispersion in Aqueous Solution at Extraordinarily High Solids Concentrations

Journal
Langmuir, 34(39)

ISSN
0743-7463

Authors
Guo, Yijun
Mishra, Manish K
Wang, Futianyi
et al.

Publication Date
2018-10-02

DOI
10.1021/acs.langmuir.8b01898

Peer reviewed

LANGMUIR Article
Cite This: Langmuir 2018, 34, 11738−11748
pubs.acs.org/Langmuir

Hydrophobic Inorganic Oxide Pigments via Polymethylhydrosiloxane Grafting: Dispersion in Aqueous Solution at Extraordinarily High Solids Concentrations

Yijun Guo,[†] Manish K. Mishra,[†] Futianyi Wang,[†] Joseph Jankolovits,[†] Ahmet Kusoglu,[‡] Adam Z. Weber,[‡] Ant Van Dyk,[§] Kebede Beshah,*[,§] James C. Bohling,[§] John A. Roper III,[§] Clayton J. Radke,[†] and Alexander Katz*[,†]

[†]Department of Chemical and Biomolecular Engineering, University of California, Berkeley, California 94720-1462, United States
[‡]Energy Conversion Group, Lawrence Berkeley National Laboratory, MS 70-108B, 1 Cyclotron Road, Berkeley, California 94720, United States
[§]The Dow Chemical Company, Midland, Michigan 48674, United States

S *Supporting Information*

ABSTRACT: Building on the recent demonstration of aqueous-dispersible hydrophobic pigments that retain their surface hydrophobicity even after drying, we demonstrate the synthesis of surface-modified Ti-Pure R-706 (denoted R706) titanium dioxide-based pigments, consisting of a thin (one to three monolayers) grafted polymethylhydrosiloxane (PMHS) coating, which (i) are hydrophobic in the dry state according to capillary rise and dynamic vapor sorption measurements and (ii) form stable aqueous dispersions at solid contents exceeding 75 wt % (43 vol %), without added dispersant, displaying similar rheology to R706 native oxide pigments at 70 wt % (37 vol %) consisting of an optimal amount of conventional polyanionic dispersant (0.3 wt % on pigment basis). The surface-modified pigments have been characterized via ^{29}Si and ^{13}C cross-polarization/magic angle spinning solid-state NMR spectroscopy; infrared spectroscopy; thermogravimetric and elemental analyses; and ζ potential measurements. On the basis of these data, the stability of the surface-modified PMHS-R706 aqueous dispersions is attributed to steric effects, as a result of grafted PMHS strands on the R706 surface, and depends on the chaotropic nature of the base used during PMHS condensation to the pigment/polysiloxane interface. The lack of water wettability of the surface-modified oxide particles in their dry state translates to improved water-barrier properties in coatings produced with these surface-modified pigment particles. The synthetic approach appears general as demonstrated by its application to various inorganic-oxide pigment particles.

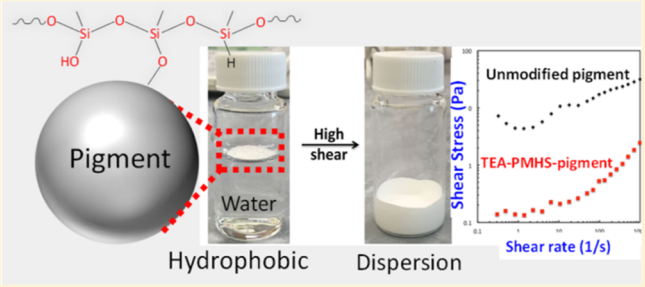

INTRODUCTION

The fundamental challenges posed by the design and synthesis of inorganic-oxide particles for aqueous dispersions in paints and coatings formulations (which account for over 3 million tons of titanium dioxide pigment used each year) seem mutually incompatible and, as a result, unachievable.[1,2] On the one hand, coatings with improved water-barrier properties require incorporation of hydrophobic character into the pigment,[3,4] whereas aqueous dispersion stability for reduced aggregation and improved opacity requires hydrophilic functional groups, which in the past has been accomplished via incorporation of anionic surface charge into the paint pigment.[5−7] To endow aqueous dispersibility to hydrophobic inorganic-oxide particles, research has focused on pigment encapsulation, such as with polymer shells,[8,9] adsorbed latices,[10] or multilayers.[11] Recently, hydrophobic surface modification of pigment particles with alkylsilane monolayers and adsorbed polyanion dispersants has led to stable aqueous dispersions,[12] and we have recently demonstrated that hydrophobically surface-modified pigment composites consisting of adsorbed polyanions remain hydrophobic even after drying the aqueous dispersion, which leads to reduced water adsorption and improved hydrophilic stain resistance in coating films comprising these composites.[13] However, the challenge of aqueous dispersion of particles that are hydrophobic upon drying persists, particularly so at the high solids concentrations that are typically required for coatings applications,[14] exceeding 37 vol % (70 wt % pigment) solids. Indeed, obtaining aqueous dispersions of hydrophobically modified pigments at these high solids concentrations has been difficult because of the tendency of stabilizing additives to degrade hydrophobicity and for hydrophobically modified

Received: June 7, 2018
Revised: August 24, 2018
Published: August 28, 2018

DOI: 10.1021/acs.langmuir.8b01898
Langmuir 2018, 34, 11738−11748

particles to aggregate into flocs or gels if they are not sufficiently stabilized by steric and electrostatic repulsion, leading also to high viscosities (i.e., undesirable rheological characteristics).[12,13]

Here, we describe the synthesis and characterization of hydrophobically modified pigment particles that do not require any additives for their dispersion in aqueous solution, even at high solids fractions exceeding 43 vol % (75 wt % for TiO_2-based pigments) and, crucially, which, upon drying, retain the hydrophobicity that they exhibited in their dry form prior to aqueous dispersion. Our synthetic approach relies on amine-catalyzed polymethylhydrosiloxane (PMHS) grafting to the pigment surface, yielding hydrophobically modified pigments that form low-viscosity, stable dispersions at high solids concentrations in water. We demonstrate this approach with a commercial pigment, Ti-Pure R-706 (denoted R706), comprised of a ∼275 nm diameter titanium dioxide rutile core and a ca. 3−5 nm thick aluminosilicate shell.[16] Central to our study is a comparison of two amine catalysts for PMHS condensation consisting of triethylamine (TEA) and 2-amino-2-methyl-1-propanol (AMP), which lead to tightly adsorbed monolayers of amines at the pigment/polysiloxane interface and drastically different grafted PMHS layers on the pigment surface, in terms of the proportion of flexible versus rigidly anchored PMHS chains. We also extend our approach to other inorganic-oxide pigment surfaces, such as Kronos 2310 and Tiona 595, which are similarly sized to R706 but consist of either a chloride process rutile titanium dioxide pigment (Tiona 595) or an oxide overlayer consisting of alumina, silica, and zirconia (Kronos 2310), which demonstrates the generality of our synthetic approach.

EXPERIMENTAL SECTION

PMHS, acetone, hexane, 2-amino-2-methyl-1-propanol $(CH_3)_2C(NH_2)CH_2OH$ (AMP), poly(acrylic acid) (PAA) solution ($[-CH_2CH(COOH)-]_n$; average M_w ∼ 2000, 50 wt % in H_2O, electronic grade) were purchased from Aldrich. Triethylamine $N(CH_2CH_3)_3$ (TEA) was purchased from Fisher Scientific. Triton X-100 (646.85 g/mol) was purchased from Acros Organics. Commercial polyelectrolyte co-polymer dispersants consisting of TAMOL 1124 (consisting of a low molecular-weight hydrophilic co-polymer containing carboxylic acid functionality) and OROTAN CA-2500V (consisting of a low-molecular-weight hydrophobic co-polymer containing carboxylic acid functionality) were obtained from the Dow Chemical Company. Ti-Pure R-706 (R706) comprises an ∼275 nm diameter particle core that is coated with an ca. 3−5 nm thick aluminosilicate overlayer shell, and was obtained from the Chemours Company.[16]

Rheology measurements were performed on a cone-and-plate viscometer (Carri-Med rheometer, CSL^2 500) with a 4 cm diameter an 2° cone angle at 23 °C. Thermogravimetric analysis (TGA) was performed on a Netzsch 449C Jupiter TGA in a mixed-gas flow consisting of 20 vol % O_2 and 80 vol % Ar. The temperature program consisted of: (i) heating at 5 °C/min to 120 °C and holding there for 60 min, followed by (ii) heating at 5 °C/min to a final temperature of 800 °C.

N_2 physisorption at 77 K and capillary-rise measurements were performed according to the procedures described previously.[13]

Synthesis of TEA-PMHS-R706. In a 1 L round-bottom flask, 250 g of R706 was combined with 2.5 mL of TEA, 2.5 mL of TAMOL 1124, and 500 mL of water and stirred at 2500 rpm with a mechanical stirrer at room temperature for a period of 1 h so as to result in an aqueous slurry of pH 10.8. Under stirring, 25 mL of PMHS was subsequently added into the reaction mixture via a syringe pump at a rate of 1.5 mL/h. This mixture was stirred overnight at room temperature at a stirring rate of 2500 rpm. The suspension was centrifuged, and the solid was isolated by decanting the supernatant. The sample was subsequently washed by suspending the solids in 300 mL of deionized (DI) water via vortexing (2 min) and sonication (3 min). The solid was then recovered via centrifugation and subsequently washed again with water, followed by two washes with acetone and a final wash with mixed hexanes. The solid was dried under vacuum overnight and ground to a fine white powder with a mortar and pestle; yield = 251.5 g. All of the TEA-PMHS-R706 samples in this manuscript were synthesized according to the procedure described above, except for the sample used for the preparation of paint films. That one sample was prepared in a way that led to a wet cake final product, as opposed to the dry powder above. This sample was prepared identically up to and including the first water wash. Then, afterward, instead of washing with water again as above, the sample was subsequently washed with acetone, hexane, acetone, and two additional water washes. After the final water wash, the sample was centrifuged and the supernatant was decanted. The wet cake was collected and stored in a sealed glass bottle. For all of the washes above, the volume of each wash was approximately 300 mL.

Synthesis of AMP-PMHS-R706. In a 1 L round-bottom flask, 250 g of R706 was combined with 5.3 mL of 2-amino-2-methyl-1-propanol (AMP), 2.5 mL TAMOL 1124, and 500 mL of water and stirred at 2500 rpm with a mechanical stirrer at room temperature for a period of 1 h so as to result in an aqueous slurry of pH 10.8. Under stirring, 25 mL of PMHS solution was subsequently added into the reaction mixture via a syringe pump at a rate of 1.5 mL/h. This mixture was stirred overnight at a stirring rate of 2500 rpm at room temperature. The suspension was centrifuged, and the solid was isolated by decanting the supernatant. The sample was subsequently washed by suspending the solids in 300 mL of deionized water via vortexing (2 min) and sonication (3 min). The solid was then recovered via centrifugation and subsequently washed again with water, followed by two washes with acetone and a final wash with mixed hexanes. The solid was dried under vacuum overnight and ground to a fine white powder with a mortar and pestle; yield = 248.9 g.

Synthesis of Ammonia-PMHS-R706. The synthesis was conducted exactly as described above for AMP-PMHS-R706, except that 14 mL of concentrated aqueous ammonium hydroxide (14.6 M) was used instead of the AMP; yield = 249.4 g.

Synthesis of KOH-PMHS-R706. The synthesis was conducted exactly as described above for AMP-PMHS-R706, except that 3 mL of aqueous KOH (10 M) was used instead of the AMP; yield = 249.2 g.

Synthesis of TEA-PMHS-R706(PAA). In a 1 L round-bottom flask, 250 g of R706 was combined with 3.5 mL of TEA, 2.5 mL of PAA, and 500 mL of water and stirred at 2500 rpm with a mechanical stirrer at room temperature. The resulting aqueous slurry was measured to have a pH of 10.8. All subsequent steps followed the synthesis of AMP-PMHS-R706; yield = 248.4 g.

Synthesis of PMHS-R706 (No Amine). As an additional control, we synthesized a surface-modified pigment in the absence of a base catalyst, using only deionized water as solvent (i.e., no amine or KOH was used). This procedure follows the one above for AMP-PMHS-R706, except in the absence of AMP; yield = 248.5 g.

Capillary-Rise Measurements. Capillary-rise testing is performed by packing a column of the dry powdered material to be tested and measuring the height of a 2.5 mM bromothymol blue solution in 0.25 mM pH 8 aqueous *N*-(2-hydroxyethyl)piperazine-*N*′-ethanesulfonic acid in a packed column after 225 min. The advancing contact angle is calculated based on the measured height using a previously reported equation,[13] assuming a θ value of 50° for R706.

Solid-State NMR Spectroscopy. Solid-state NMR spectroscopy experiments were performed on an AVANCE III Bruker spectrometer; 7 and 4 mm solid-state NMR probes were used for ^{29}Si and ^{13}C cross-polarization (CP) experiments, respectively, with a variable-amplitude spin-lock level. Typically, about 450−470 mg of a dry powdered sample was used for the ^{29}Si experiment. Magic angle spinning (MAS) rates were typically 6 kHz for the 7 mm probe and 14 kHz for the 4 mm probe, and about 40 000 scans were acquired for

DOI: 10.1021/acs.langmuir.8b01898
Langmuir 2018, 34, 11738−11748

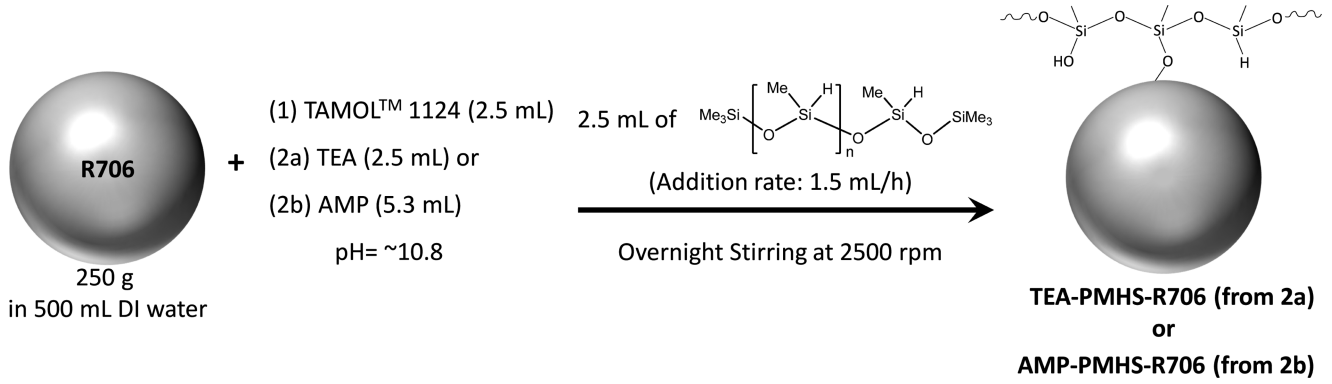

Figure 1. Schematic diagram showing the overall reaction of PMHS grafting on the surface of R706.

each CP experiment. The signal for the Q components of the silica in R706 centered at −100 ppm and was used as an internal reference for the chemical shifts, and for semiquantitative intensity comparisons of the ^{29}Si spectra.

ζ Potential Measurements. Electrokinetic measurements were conducted using a Malvern Nano-Zetasizer equipped with a high-concentration ζ cell. All liquid solvents were filtered through a 0.2 μm syringe filter prior to use for making dispersions. Homogeneous dispersions of the hydrophobic-grafted PMHS-modified R706 were obtained in water with the aid of sonication. The electrokinetic pH profile of the particles was measured on a 0.01 mg/mL suspension of the particles in 0.1 mM aqueous sodium chloride, consistent with previously used salt concentrations for measurement of surface charge.[13] The pH was adjusted to the desired value with sodium hydroxide or hydrochloric acid. The samples were sonicated for 5−10 min prior to the ζ potential measurement.

Preparation of the Dispersions. Pigment, water, ammonium hydroxide, and dispersant (if required) were combined at appropriate levels in a 10 mL plastic mixing cup (FlackTek) to obtain a 53.5 vol % (82 wt % for R706) pigment concentration. Using a dual-asymmetric centrifuge (FlackTek 150.1 FVZ Speedmixer), the sample was mixed for 2 min at 1700 rpm, yielding a thick white paste. Two ceramic grinding beads were utilized for the hydrophobically modified pigments. Subsequently, water was added to dilute the sample to the appropriate pigment-volume concentration. The sample was then additionally mixed in a dual-asymmetric centrifuge for 3 min at 3500 rpm. If necessary, aqueous 6 M ammonium hydroxide or 4 M hydrochloric acid was added in small amounts (1−10 μL) to adjust the pH, followed by further mixing for 1 min at 2000 rpm. The samples were placed on an orbital shaker for 14−24 h before rheology measurements were collected.

Dynamic vapor sorption (DVS) measurements of the powders were conducted using a DVS analyzer with temperature and humidity control (Surface Measurement Systems, U.K.). The powders were placed onto a glass sample pan and attached to the weight balance of the DVS. The samples were first dried at 120 °C for 1 h to remove moisture and determine its dry mass, M_0. The samples were then cooled to 25 °C, equilibrated for 30 min, and then humidified by maintaining in 90% relative humidity (RH) air for 6 h, followed by a dehumidification step back to 0% RH. The mass change in each sample due to vapor sorption/desorption, ΔM, was recorded every second without interruption between the steps. The change in the mass was normalized to the dry mass, when calculating the percent mass change, or $\Delta M/M_0 \times 100$. Prior to each experiment, the sample pans were cleaned with hexane, acetone, and DI water and then air-dried.

RESULTS AND DISCUSSION

Impact of PMHS Grafting on Pigment Hydrophobicity. Figure 1 schematically illustrates our approach for grafting PMHS onto R706, a commercial titanium dioxide pigment consisting of a 275 nm rutile core and 3−5 nm aluminosilicate shell.[16] An organic base, such as either TEA or AMP, maintained a pH of 10.8 and facilitated the condensation of PMHS with surface hydroxyl functionalities of the native pigment particles. The resulting surface-modified pigment particles consist of PMHS strands that are grafted onto hydroxyl OH functional groups present on the native oxide surface of the aluminosilicate overlayer. We also investigated other bases that are known to promote the grafting of PMHS grafting to inorganic oxide and, in particular, silica surfaces,[17−19] such as ammonia and potassium hydroxide, but, as discussed below, these led to hydrolytically unstable hydrophobic coatings (vide infra). To assess the degree of hydrophobicity in the resulting surface-modified pigments in their dry state, capillary-rise measurements were used to estimate the advancing water/air contact angle.[20] This was performed on both the as-synthesized powder after drying and surface-modified pigment that underwent a prior stress test that consisted of high-shear mixing (which maximizes the rate of water transport and the pinning of water to the pigment external surface)[21] of an aqueous dispersion of the surface-modified pigment, prior to its drying. The latter stress test was meant to characterize the hydrolytic stability of the hydrophobically modified surface to high-shear mixing conditions, at a pH of 8.7, which is typical for paints and coatings, commonly in the range of 8.5−9.5.[22] Invariance in the water contact angle for the surface-modified R706 pigment after high-shear mixing demonstrates hydrolytic stability of the grafted PMHS coating—an absolutely essential quality for applications of surface-modified pigment particles.

Capillary-rise height measurements are summarized in Table 1. Contact angles are based on the reasonable assumption of a water contact angle for native R706 of 50°,[23,24] and demonstrate a hydrophobic (contact angle >90°) PMHS surface-modified pigment when using an organic base as catalyst, such as either TEA or AMP, corresponding to a capillary-rise height of 0.03 ± 0.02 cm for TEA-PMHS-R706 and 0.04 ± 0.02 cm for AMP-PMHS-R706, compared to 1.56 ± 0.01 cm for unmodified R706. The hydrophobicities of TEA-PMHS-R706 and AMP-PMHS-R706 are similar to that previously observed,[25] based on grafting PMHS to a glass slide, where an increase in the water contact angle from 30° to 97° was observed upon surface modification with PMHS. Similar hydrophobicity has been reported in macroporous silica films that were synthesized by a combination of PMHS and hexamethydisilazane,[26] which exhibit water/air contact angles of up to 112°.

DOI: 10.1021/acs.langmuir.8b01898
Langmuir 2018, 34, 11738−11748

Table 1. Capillary-Rise Testing of Hydrophobicity of Various Materials[a]

material	h (cm)	θ (deg)
R706	1.56 ± 0.06	50
R706 after high-shear mixing stress test[a]	>1.56	<50
PMHS-R706 (no amine)	0.03 ± 0.02	≥90
PMHS-R706 (no amine) after high-shear mixing stress test[a]	1.36 ± 0.16	61
TEA-PMHS-R706	0.03 ± 0.02	≥90
TEA-PMHS-R706 after high-shear mixing stress test[a]	0.06 ± 0.02	≥90
AMP-PMHS-R706	0.04 ± 0.02	≥90
AMP-PMHS-R706 after high-shear mixing stress test[a]	0.07 ± 0.03	≥90
ammonia-PMHS-R706	0.21 ± 0.07	89
ammonia-PMHS-R706 after high-shear mixing stress test[a]	0.83 ± 0.14	79
KOH-PMHS-R706	0.32 ± 0.09	88
KOH-PMHS-R706 after high-shear mixing stress test[a]	1.16 ± 0.15	69
TEA-R706	>1.56	<50
AMP-R706	>1.56	<50

[a]High-shear mixing stress test performed at pH 8.7.

To assess the role of residual amounts of amine base (TEA and AMP) on the observed hydrophobicity, control materials consisting of TEA-R706 and AMP-R706 were synthesized. These controls were synthesized by the same procedure as for the corresponding PMHS-containing materials, TEA-PMHS-R06 and AMP-PMHS-R706, except that no PMHS was added. Thus, controls TEA-R706 and AMP-R706 consist solely of physisorbed amine that remains behind despite the extensive water, acetone, and hexane washes (the actual amount of residual amine in these control and grafted PMHS materials was quantified vide infra). Data in Table 1 demonstrate that residual amine in TEA-R706 and reported AMP-R706 does not render hydrophobicity. We conclude that the pigment hydrophobicity in Table 1 is due to grafted PMHS on the R706 surface.

Hydrophobicities of surface-modified pigments TEA-PMHS-R706 and AMP-PMHS-R706 after a high-shear mixing stress test are discussed below. When using an inorganic base, such as either KOH or aqueous ammonia in the grafted PMHS synthesis, reduced hydrophobicity was observed for the surface-modified pigment, in the range of water contact angles of 88−89°. Further, these surface-modified pigment particles were not stable to the high-shear mixing stress test, as a further degradation in the water contact angle in the range of 69−79° was observed, toward the range observed for the unmodified R706 control. Similar poor results were obtained in the absence of a base catalyst, which is demonstrated in Table 1. This is in contrast to both TEA-PMHS-R706 and AMP-PMHS-R706, which maintain the same capillary-rise characteristics, amounting to the same degree of hydrophobicity, after the high-shear mixing stress test as well as storage, even when storing these samples at 100% relative humidity for 3 weeks at room temperature prior to testing. Altogether, these data demonstrate hydrolytically stable grafted PMHS coatings in TEA-PMHS-R706 and AMP-PMHS-R706, and we thus focused on these two materials as potentially promising leads. While all bases achieved the same pH of ∼9.8 during synthesis of the grafted PMHS coating, our observations indicate that the more chaotropic (weakly hydrated) the base used, the more stable the hydrophobicity of the PMHS coating after a high-shear mixing stress test. We interpret this to mean that with the more kosmotropic inorganic bases, PMHS condensation is less effective, which creates a less hydrolytically stable hydrophobic overlayer on the R706 pigment. Such a trend would be supported by the thinner overlayer achieved with the primary amine in AMP as base, compared to the more chaotropic, tertiary amine in TEA. In previously reported systems consisting of bases in close proximity (<1 nm) to hydrophobic functional groups, it has been shown that the nature of the base can have a profound effect on the strength of hydrophobic interactions involving the functional groups.[27] We hypothesize that these interactions could in fact have a strong influence on the condensation kinetics involving PMHS and the underlying pigment oxide surface.

Stable Aqueous Dispersions of PMHS-Modified R706 up to 75 wt % (43 vol %). Previously, we reported the synthesis of hydrophobically modified pigment, which consisted of TMS-capped R706.[13] When preparing concentrated aqueous dispersions of these hydrophobically modified pigments, to obtain liquid dispersions, the solids content was held in the range of 50 wt % (20 vol %) pigment in aqueous suspension.[13] In particular, at higher TMS-capped R706 contents of 70 wt % (37 vol %) or above in aqueous suspension, pastes as opposed to liquid dispersions were obtained, even in the presence of added polyanion dispersants. Yet obtaining liquid aqueous dispersions at these high solids concentrations is essential for applications, which commonly involve transport of pigment in the wet state at these solids levels. These solids levels begin to approach but are still below the theoretical maximum for noninteracting spherical particles of 49.4 vol % (80 wt % for R706).[14,28] The challenge of dispersing pigment at these solids levels involves avoiding pigment-particle aggregation into flocs or gels, which can occur if they are not sufficiently stabilized by either steric or electrostatic effects.[12,15]

We, therefore, investigated dispersions of PMHS-modified pigments at higher solids levels, in the range of 70−75 wt % (37−43 vol %) solids. This was performed by first dispersing TEA-PMHS-R706 and AMP-PMHS-R706 in water at pH 8.7 ± 0.1 with a high-shear mixer, at 82.5 wt % (53.5 vol %), followed by dilution to the desired solids concentration prior to subjecting the sample to a second cycle of high-shear mixing. At all concentrations of up to 75 wt % (43 vol %), both TEA-PMHS-R706 and AMP-PMHS-R706 yielded fluid dispersions. In stark contrast, unmodified R706, while forming liquid-like suspensions at low solid weight percentages of 50 wt % (20 vol %), formed a gelatinous paste above 70 wt % (37 vol %). This indicates extensive particle aggregation in R706 at these higher solids contents.

Assessment of dispersion stability was performed via viscometry, on high solids aqueous suspensions of R706, TEA-PMHS-R706, and AMP-PMHS-R706. Data shown in Figure 2a represent aqueous suspensions at 70 wt % (37 vol %) and pH 8.7, in the absence of added dispersant. Under these conditions, the suspension of R706 displays a high yield stress of 7 Pa, evident at a low shear rate of 0.3 s^{-1}, which arises from particle aggregation in solution.[29,30] Thus, in the absence of added dispersant, the rheology of R706 is consistent with strong interparticle attraction, akin to that observed in the gelatinous paste describe above. Under the same conditions as in Figure 2a, TEA-PMHS-R706 and AMP-PMHS-R706 dispersions exhibit apparent viscosities of 8.8 × 10^{-3} and 7.1

DOI: 10.1021/acs.langmuir.8b01898
Langmuir 2018, 34, 11738−11748

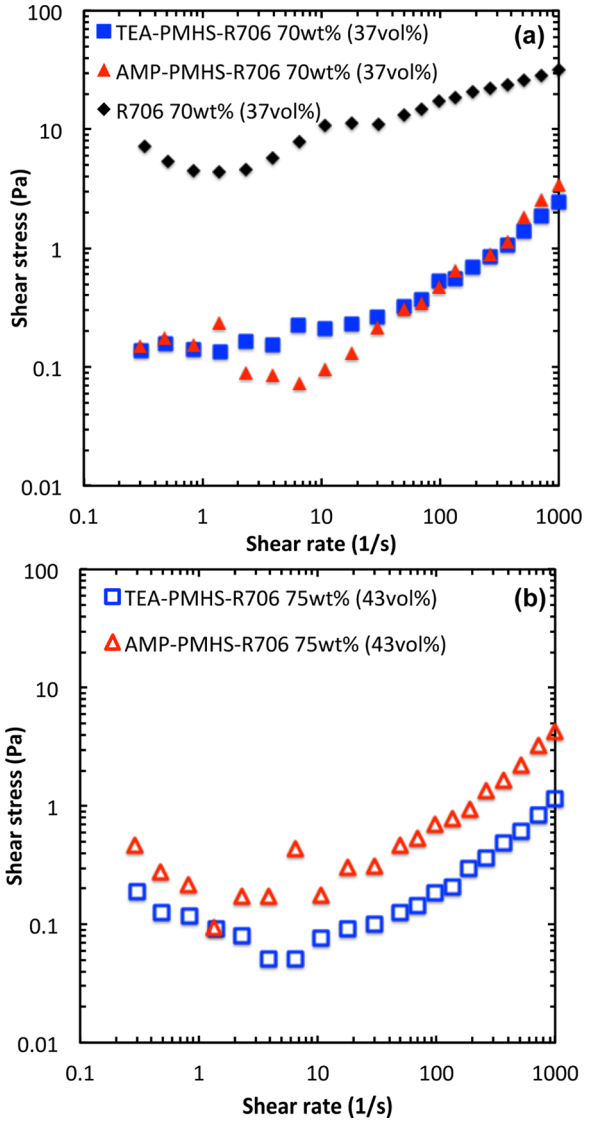

Figure 2. Rheology of 70 wt % (37 vol %) or 75 wt % (43 vol %) particle suspensions consisting of either R706 or surface-modified R706 with PMHS, in water at pH 8.7.

$\times 10^{-3}$ Pa s, respectively, at a low shear rate of 30 s^{-1}, and equally low yield stresses of 0.14 and 0.15 Pa, respectively. These viscosities are lower than values previously measured for hydrophobically modified silicas dispersed in water with polymer and polanionic dispersants, at lower solids volume fractions.[9,12] For both PMHS-modified pigments, the yield stress further reduces to below 0.1 Pa with a small amount (0.025 wt % relative to pigment weight) of nonionic surfactant (Triton X-100, Dow),[29−31] commonly used in commercial paints and coatings formulations (see Figure S2).[32,33] The distinctly low apparent viscosities (only 8-fold larger apparent viscosity for 70 wt % (37 vol %) concentrated solids suspension compared to water) and low yield stresses below 1 Pa in TEA-PMHS-R706 and AMP-PMHS-R706 at high solids dispersion demonstrate the improved dispersion stability afforded by PMHS grafting onto the R706 pigment particle.

We also dispersed TEA-PMHS-R706 and AMP-PMHS-R706 particles at an even higher solids concentration of 75 wt % (43 vol %) and also obtained similar low-viscosity liquid dispersions for both. Indeed, data shown in Figure 2b demonstrate that the 43 vol % suspensions of TEA-PMHS-R706 and AMP-PMHS-R706 particles possess nearly identical apparent viscosities compared to the 37 vol % suspension. For TEA-PMHS-R706, the yield stress (as measured below shear rates of 5 s^{-1}) is nearly the same for both concentrations of suspension, below 0.2 Pa, whereas AMP-PMHS-R706 exhibits a 3-fold higher yield stress at 75 wt % (43 vol %) relative to a suspension at 70 wt % (37 vol %). The observed local minimum in the shear stress versus shear rate profiles for both TEA-PMHS-R706 and AMP-PMHS-R706 in Figure 2b has been previously attributed to the breakage of small aggregates at low shear rates, followed by a colloidal shear-thickening behavior, in related colloidal dispersions. This has been previously observed to be due to a transition from a lubricated flow of near-contacting particles to the one involving a frictionally contacting network of particles.[34]

TGA and Elemental Analysis of R706 and PMHS-Modified R706 Pigments. A central question that we address is the amount of grafted PMHS in TEA-PMHS-R706 and AMP-PMHS-R706—the two hydrophobically modified materials that demonstrated dispersion in water at 43 vol % (75 wt %). We thus characterized R706, TEA-PMHS-R706, and AMP-PMHS-R706 via Si inductively coupled plasma mass spectrometry (ICP-MS) and carbon elemental analysis, as well as TGA to understand further PMHS grafting to the pigment surface, when using different amine catalysts.

Si ICP-MS and carbon elemental analysis data are summarized in Table S1. Compared to the baseline 1.3 wt % Si content of R706, TEA-PMHS-R706 exhibited 1.0 wt % more Si, which is attributed to the PMHS coating; this number was 0.2 wt % for AMP-PMHS-R706. Because the Si content of PMHS is 47 wt %, this amounts to a PMHS coating of approximately 2.1 and 0.4 wt % for TEA-PMHS-R706 and AMP-PMHS-R706, respectively, if neglecting the grafting effects of the coating on the pigment surface (i.e., assuming the same repeat unit in the coating as in the main chain of the PMHS polymer). On the basis of this observation and the fact that the carbon content of PMHS is 20 wt %, we estimate a predicted carbon mass loading above R706 background of 0.4 and 0.1 wt % for TEA-PMHS-R706 and AMP-PMHS-R706, respectively. These estimates agree reasonably well with the measured carbon elemental analysis data in Table S1 of 0.5 wt % increase (for TEA-PMHS-R706) and 0.1% increase (for AMP-PMHS-R706). Although there is a small amount of residual amine catalyst (used for PMHS grafting) remaining chemisorbed to the pigment surface in these two materials, their amounts are too small (vide infra) to influence the carbon elemental analysis comparison above, particularly given the inherent experimental uncertainty in the latter.

Raw TGA data for R706 shown in Figure 3 demonstrate a small 1.2% weight loss between 120 and 800 °C, which is attributed to combustion of organic surface modifiers known to be present, as well as to the possibility of some surface OH condensation within the ca. 3−5 nm thick aluminosilicate shell, on the R706 pigment surface. In comparison, AMP-PMHS-R706 showed a similar weight loss to unmodified R706, corresponding to 1.1% in the same temperature window of 120−800 °C during TGA. This is not a surprising result because of the small weight change when replacing methyl $-CH_3$ functional groups present on the PMHS repeat unit (combusts to CO_2 and H_2O) with −OH functional groups during combustion. That is to say, the similar molecular weights of the $-CH_3$ and −OH functional groups could make

DOI: 10.1021/acs.langmuir.8b01898
Langmuir 2018, 34, 11738−11748

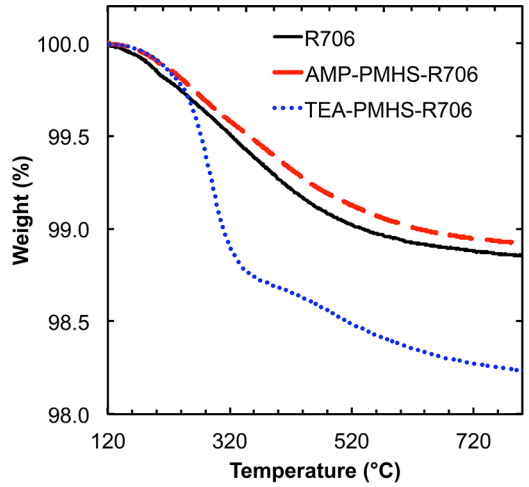

Figure 3. Thermogravimetric analysis of R706 (solid black line), TEA-PMHS-R706 (dotted blue line), and AMP-PMHS-R706 (dashed red line) in a mixture of Ar and O_2.

it difficult to observe weight change during combustion of the PMHS coating during thermogravimetric analysis in air.

Compared to AMP-PMHS-R706, we observed a larger weight loss for TEA-PMHS-R706, which exhibited a 1.8 wt % change between 120 and 800 °C. Further, the majority (1.1 wt %) of weight loss occurred in a narrow temperature window between 230 and 370 °C. That is, when normalizing the TGA at 370 °C and examining the TGA trace above 370 °C, the traces for R706, TEA-PMHS-R706, and AMP-PMHS-R706 all appear identical (see Figure S6, Supporting Information).

To gain further insight into the source of the observed weight loss for the TEA-PMHS-R706 pigment, we performed TGA on neat PMHS as a control. The outcome of TGA on neat PMHS showed a sensitivity to the gas flow rate in terms of TGA behavior, an outcome consistent with transport limitations. At low gas flow rates, when performing the experiment in a muffle furnace, only 25 ± 5% weight loss was observed. At the higher gas flow rates used during TGA of the pigments described above, over 95% of weight loss was observed for neat PMHS (see Figure S7, Supporting Information), whereas using half of the gas flow rate during TGA of neat PMHS resulted in an intermediate weight loss of 45 ± 5%. In all cases, the temperature window for the weight loss coincided with that observed for the major weight loss process in TEA-PMHS-R706, to be between 230 and 370 °C.

On the basis of the gas flow rate dependence on the observed weight loss during TGA of neat PMHS, we infer that the observed weight loss during TGA of neat PMHS is the result of evaporation rather than combustion of free PMHS fragments. Fragmentation of the original PMHS strand can occur due to cleavage of Si−O−Si bonds along the main PMHS backbone at high temperatures. This cleavage can be driven by steam synthesized during methyl-group combustion at these elevated temperatures and can cause the synthesis of shorter PMHS oligomers, which evaporate under flow conditions. Depending on the molecular weight of these shorter oligomers, evaporation could certainly be mass-transport-limited and thus dependent on the gas stream velocity during TGA.

We posit that the observed mass loss of 1.1% in the temperature window between 230 and 370 °C during TGA is the result of a combination of volatilization of PMHS fragments from the coating of TEA-PMHS-R706, as observed for the neat PMHS, as well as OH condensation processes and loss of organic modifiers (such as AMP and trimethylolpropane) associated with the R706 pigment. The latter process can be quantified by subtracting the value of 0.4 wt % change observed via TGA for R706 (AMP-PMHS-R706 has the same wt % change as R706 in this temperature window) as a baseline between 230 and 370 °C, which is commensurate with the expected amounts of organic modifiers in R706 pigment.[35] Thus, at least 0.7 wt % of the PMHS in TEA-PMHS-R706 represents a loosely grafted PMHS fragment that, while covalently attached so as to survive repetitive washes with hexane, acetone, and water during synthesis, has a loose enough attachment that it partially volatilizes in the presence of steam that is generated at high temperatures during combustion, much like neat PMHS. This freely attached PMHS fraction is expected to exhibit behavior during TGA that is intermediate between rigidly grafted PMHS, which exhibits no weight loss as surmised based on the data above for AMP-PMHS-R706, and neat PMHS, which consists of no grafting and exhibits 100% weight loss during TGA. As a result, the observed 0.7 wt % loss observed by TGA consists of a lower bound since it assumes that 100% of the freely attached grafted PMHS is volatilized. Below we further show this freely attached PMHS fraction to be uniquely present in TEA-PMHS-R706 (vide infra, see Solid-State NMR Spectroscopy of PMHS-Modified R706 Pigment section).

Solid-State NMR Spectroscopy of PMHS-Modified R706 Pigment. Based on solid-state NMR spectroscopy being a sensitive characterization technique for hybrid organic−inorganic materials,[36] ^{29}Si CP/MAS NMR spectroscopy of TEA-PMHS-R706 and AMP-PMHS-R706 was performed to characterize the microscopic state of the grafted PMHS coating, as well as to provide proof of covalent PMHS grafting via the formation of $H_3C{-}Si(OSi)_3$ connectivity. Figure 4 shows a schematic of the resonance assignments along with the spectra, which are normalized to the Q_3 and Q_4 resonances of the aluminosilicate overlayer of the pigment, in the range of −90 to −110 ppm. Resonances at −35, −57, and −64 ppm were assigned to $H{-}Si(CH_3)(OSi)_2$ (D_2^H), $HO{-}Si(CH_3)(OSi)_2$ (T_2), and $CH_3{-}Si(OSi)_3$ (T_3), in accordance with previous literature.[37−40] The presence of T_3 resonances in both TEA-PMHS-R706 and AMP-PMHS-R706 provides direct proof of PMHS chemical grafting onto the pigment surface. Both TEA-PMHS-R706 and AMP-PMHS-R706 exhibit similar normalized intensities corresponding to T_2 and T_3 resonances, implying a similar amount of grafted PMHS sites and hydrolyzed $HO{-}Si(CH_3)(OSi)_2$ functional groups in both base materials. Where the two materials differ drastically is in the greater intensity of the D_2^H region for the TEA-PMHS-R706 pigment, which has an overall integrated intensity in this region that is approximately twice as large as that for AMP-PMHS-R706. The presence of the D_2^H band for TEA-PMHS-R706 in Figure 4b,d is confirmed via diffuse-reflectance infrared Fourier transform spectroscopy, by a characteristic Si−H band at 2167 cm^{-1} (Figure S8 in the Supporting Information). A further zoom in on the D_2^H region is shown in Figure 4d for the two PMHS-modified pigments. The broad resonance at −37 ppm for AMP-PMHS-R706 is consistent with the grafted PMHS being rigidly immobilized and having hindered mobility and motion on the NMR time scale. Conversely, for TEA-PMHS-R706, in addition to having a similar intensity envelope corresponding to this broad

DOI: 10.1021/acs.langmuir.8b01898
Langmuir 2018, 34, 11738−11748

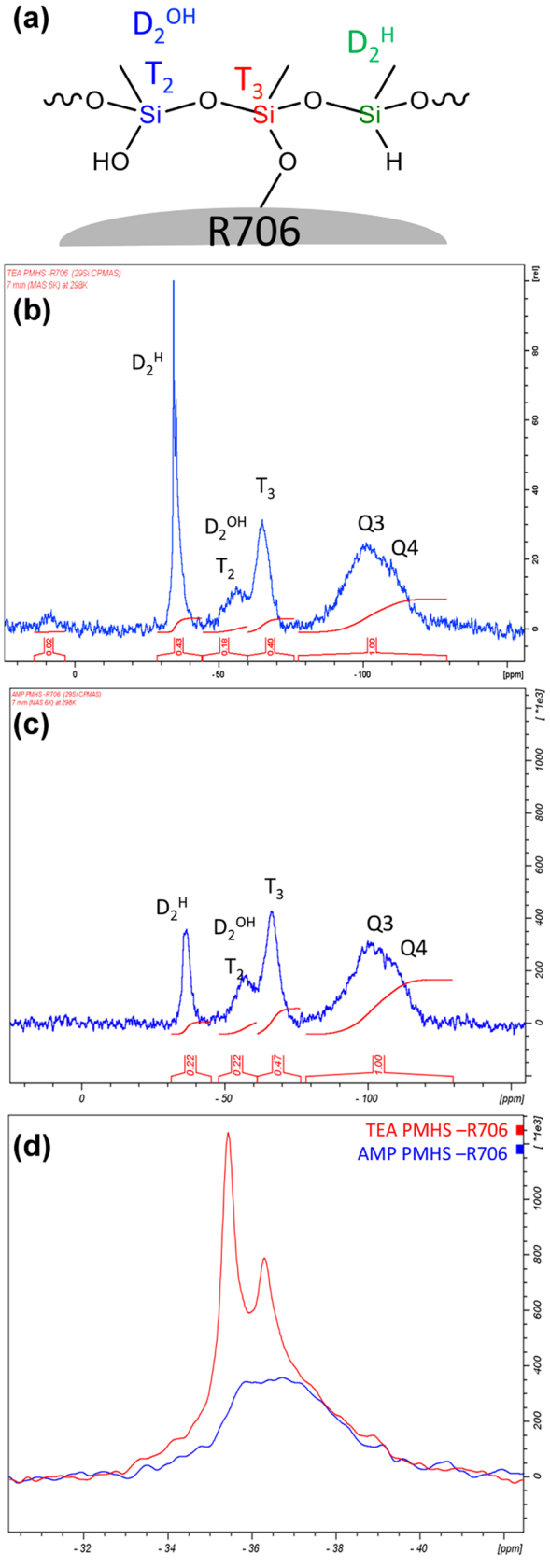

Figure 4. (a) Schematic labeling of unique Si atoms on grafted PMHS to facilitate ^{29}Si NMR peak assignments. ^{29}Si CP/MAS NMR spectroscopy of surface-modified pigments consisting of (b) TEA-PMHS-R706, (c) AMP-PMHS-R706, and (d) zoomed-in region of spectrum in (b) and (c) in the region of the D_2^H resonance.

resonance, there is an additional envelope corresponding to two sharp resonances in Figure 4d. One of these sharp resonances is centered at a chemical shift of −35.8 ppm, while the other is also sharp and centered at −36.2 ppm. Leveraging evidence of loosely bound grafted PMHS strands from TGA, we surmise that these two sharp resonances correspond to a loosely bound fraction of grafted PMHS in TEA-PMHS-R706, with the sharpness of these two resonances consistent with their high mobility on the NMR time scale. Previously, during investigations of grafted poly(dimethylsiloxane) loops on silica, large loops corresponded to sharper resonances, indicative of rapid motion.[41]

A deconvolution of the sharp and broad ^{29}Si CP/MAS resonances in the D_2^H region provides a lower-bound estimate for the amount of loosely bound PMHS, as a fraction of the total grafted PMHS in TEA-PMHS-R706. The lower-bound nature of this estimate is based on the fact that the looser-bound fraction is expected to cross-polarize with less efficiency due to its greater mobility and motion.[42] On the basis of the data in Figure 4d, deconvolution predicts that at least 26% of the D_2^H resonances are loosely bound (see Figure S9 in the Supporting Information). Further assuming that the $Si(H)CH_3$ groups are randomly distributed within the grafted PMHS strand so as to report on the strand flexibility everywhere (not clustered in a certain location), we infer that these minimum 26% of $Si(H)CH_3$ groups inform us on the fraction of PMHS strands that are loosely bound—amounting to at least 0.6 wt %. This lower-bound estimate from NMR spectroscopy can be compared to TGA data, which quantify that the weight percentage (relative to pigment) of this loosely bound fraction as at least 0.7 wt % (vide supra).

^{13}C CP/MAS spectra and resonance assignments of TEA-PMHS-R706 and AMP-PMHS-R706 are shown in Figure 5.

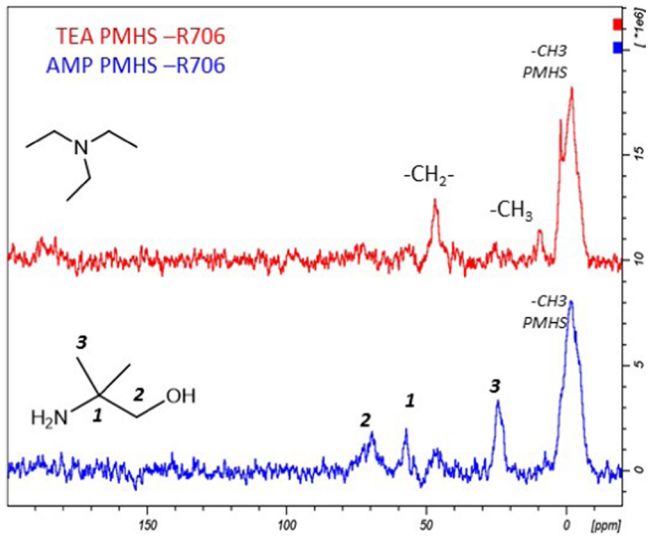

Figure 5. ^{13}C CP/MAS NMR spectra of surface-modified pigments consisting of (a) TEA-PMHS-R706 and (b) AMP-PMHS-R706.

The lack of any downfield resonances in the carbonyl region essentially rules out incorporation of TAMOL 1124 in the surface layer. A small amount of amine remaining on the pigment surface after synthesis is evident by characteristic resonances in the ^{13}C CP/MAS spectrum for both samples.

ζ Potential and Basic Site Titration. To determine the surface charge of the pigments, we measured the ζ potential as

DOI: 10.1021/acs.langmuir.8b01898
Langmuir 2018, 34, 11738−11748

a function of varying pH on unmodified R706, PMHS-modified R706, and control materials consisting of TEA-R706 and AMP-R706. Figure 6 reports the results. Previously, we

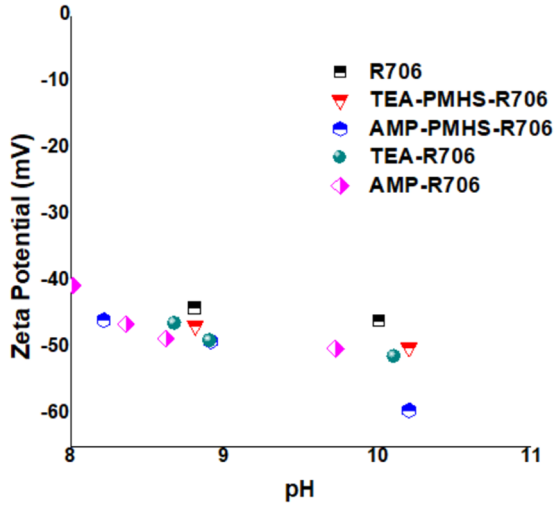

Figure 6. ζ potential vs pH for suspensions consisting of R706, TEA-PMHS-R706, AMP-PMHS-R706, TEA-R706, and AMP-R706 in 0.1 mM aqueous NaCl.

observed the importance of negative surface charge on dispersability when investigating TAMOL 1124 adsorbed on both native R706 surfaces and hydrophobically modified pigment surfaces.[13] However, in contrast, data shown in Figure 6 fail to reveal any differences in surface charge among all of the materials investigated, within the pH range of interest for aqueous dispersions. As a result, we infer that the mechanism of increased dispersibility must stem from steric stabilization[43] of the grafted PMHS strands rather than from surface charge. Generally, steric stabilization of a dispersion of colloidal particles refers to the stability of a system achieved by thermodynamic repulsion, when a polymer layer/coating on two colloidal particles cannot interpenetrate each other due to entropic barriers (i.e., the free-energy change upon interpenetration (ΔG) is positive).[44,45] Steric stabilization has been previously invoked in the dispersion of hydrophobic surface-modified silica particles.[12] In our case, we envision that the collapse of the hydrophobic PMHS chains in water contributes to the entropic origin of steric stabilization because the entropy loss for chain deformation for collapsed chains should be much smaller than for swollen chains.[46]

Nitrogen Porosimetry. Nitrogen physisorption at 77 K was used to measure the surface area change accompanying PMHS grafting; these data are summarized in Table S1 for R706, TEA-PMHS-R706, and AMP-PMHS-R706. The surface area drops from 11.4 m^2/g for R706 to 7.6 and 10.4 m^2/g for TEA-PMHS-R706 and AMP-PMHS-R706, respectively, as a result of PMHS grafting. We interpret this decrease to be due to PMHS blocking internal micropores in the ∼5 nm aluminosilicate overcoat on the particle surface and surmise that the larger concentration of flexible PMHS strands in the TEA-PMHS-R706 material facilitates this micropore blockage via collapse of these flexible strands onto the surface, in the dry state—the state of relevance for nitrogen porosimetry.

Stabilization Mechanism Scheme. Altogether, combining all of the data discussed above for characterizing TEA-PMHS-R706 and AMP-PMHS-R706, we propose a simplified schematic model of each material. We propose the latter material to consist of a rigidly attached grafted layer of PMHS on the pigment surface, whereas TEA-PMHS-R706 consists of a multilayer of grafted PMHS above and beyond this first surface layer. For all materials, PMHS grafts to the oxide particle through random irreversible chemisorption, with the high enthalpy of interaction in the first layer between condensable groups on the polymer backbone and aluminosilicate external surface hydroxyl functionality of R706 expected to generate short loops. This is consistent with the rigid layer of D_2^H resonances observed for both TEA-PMHS-R706 and AMP-PMHS-R706. We propose that the second layer in TEA-PMHS-R706 grafts as a multilayer on top of the first rigid chemisorbed PMHS layer, and is more flexible as a result of the much lower density of available hydroxyl groups, to which it can anchor. Due to the expected steric interference of the first layer blocking some of the aluminosilicate surface, the hydroxyl groups are limited to silanol groups on the existing first rigid layer—observable as T_2 resonances in the ^{29}Si NMR spectrum. On the basis of TGA, ^{29}Si and ^{13}C CP/MAS NMR spectroscopy, ζ potential measurement, acid−base back titration, and carbon analysis, we envision the PMHS anchoring of R706 surface, as illustrated in Figure 7. The steric

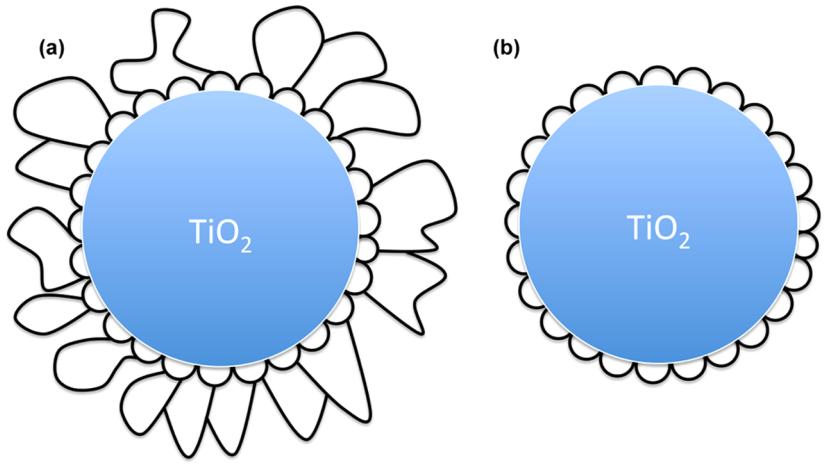

Figure 7. Schematic illustration of grafted PMHS coating in surface-modified pigments consisting of (a) TEA-PMHS-R706 and (b) AMP-PMHS-R706. The coating thickness is not drawn to the same scale as the pigment particle to enhance visual clarity.

DOI: 10.1021/acs.langmuir.8b01898
Langmuir 2018, 34, 11738−11748

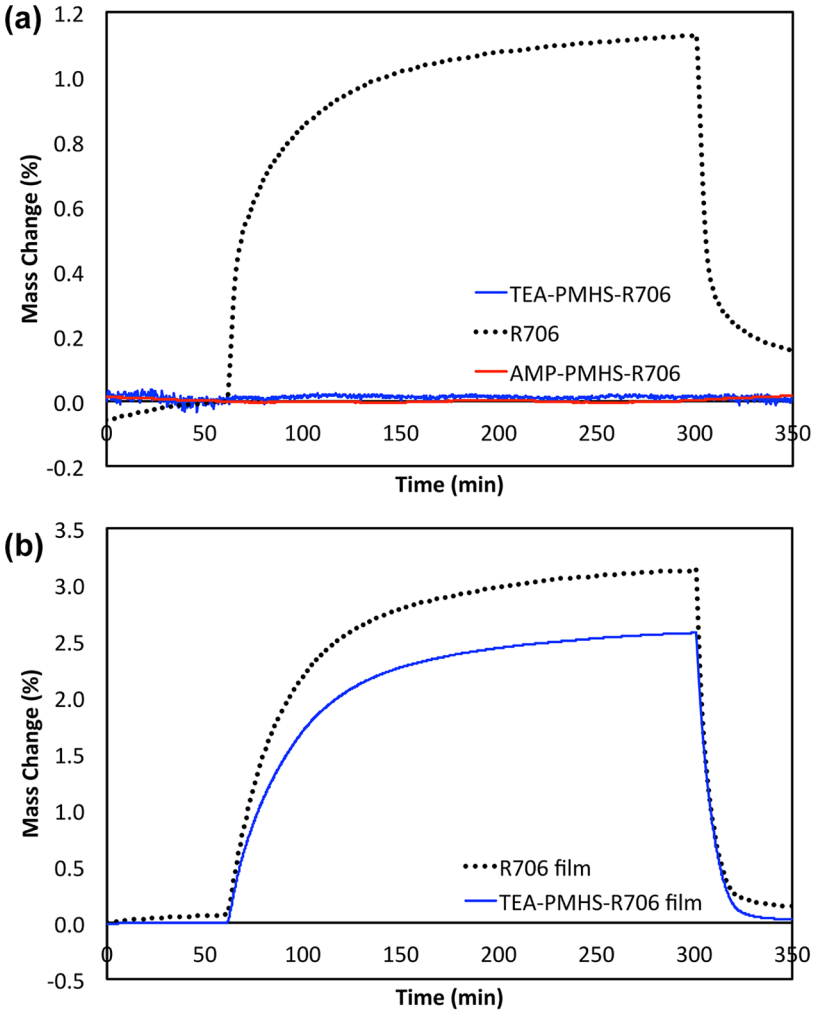

Figure 8. Dynamic vapor sorption data for (a) R706 paint film (dotted black), TEA-PMHS-R706 powder (blue line), and AMP-PMHS-R706 powder (red line) and (b) R706 paint film (dotted black) and TEA-PMHS-R706 film (blue line) plotted as the change in mass of the dry powders vs time in a dynamic atmosphere that switches between 0% humidity and 90% humidity dinitrogen. The gray dashed line indicates a switch in the flowing gas.

stabilization of grafted PMHS strands in both TEA-PMHS-R706 and AMP-PMHS-R706 is consistent with the nearly identical ζ potential for all materials in the pH range of interest for paints and coatings. In addition, the flexible component of PMHS on the TEA-PMHS-R06 particle surface generates an additional steric barrier against particle aggregation, which imparts additional stability above and beyond that envisioned in AMP-PMHS-R706. The total amount of PMHS grafted in TEA-PMHS-R706 corresponds to 1.4 wt %, with at least half of that comprising flexible rather than rigidly attached chains (vide supra). On the other hand, grafted PMHS within surface-modified pigment AMP-PMS-R706 is rigid according to ^{29}Si CP/MAS NMR spectroscopy and comprises a mass loading of approximately 0.47 wt %. This agrees reasonably well with the estimated coverage for a monolayer of grafted PMHS on R706 corresponding to the jamming limit, which predicts an approximate mass loading of 0.6 wt %.

Water-Barrier Properties. To assess the water-barrier properties of the surface-modified pigments, we examined the water uptake of dry R706, TEA-PMHS-R706, and AMP-PMHS-R706 particles via dynamic vapor sorption (DVS, see Experimental Section). Similar to what we have reported previously,[13] unmodified R706 exhibits around 0.9% weight increase after treatment at 90% humidity for 4 h. The absorption of water vapor happens quickly after R706 powder is exposed to water, nearly 90% of it occurring within the first 1 h after 90% relative humidity treatment. In stark contrast, the dynamic vapor sorption uptake of TEA-PMHS-R706 stayed nearly constant, indicating almost no water uptake under the same treatment. As seen in Figure 8, we find no appreciable water uptake on this sample. The same is true for AMP-PMHS-R706 via DVS in Figure 8a. These results mirror the lack of water wetting observed in the data of Table 1 with regard to these two materials, in contrast to unmodified R706.

The DVS data in Figure 8a prompted us to investigate a paint formulation with hydrophobically modified R706 that consists of grafted PMHS. We thus formulated TEA-PMHS-R706 into a paint formulation and compared it with a control paint synthesized with R706. These formulations were synthesized by combining pigment with RHOPLEX SG-10M (RHOPLEX SG-10M emulsion is a versatile 100% acrylic copolymer that was designed for use in high-quality interior/exterior semigloss paints) and small amounts of additives (see Table S4 for details of film formulation and paint film preparation). Two dry paint films corresponding to pigments TEA-PMHS-R706 and unmodified R706 were tested via DVS

DOI: 10.1021/acs.langmuir.8b01898
Langmuir 2018, 34, 11738−11748

using procedures identical to those used above for DVS testing of the pigment powders. Data in Figure 8b demonstrate that the paint film formulated with TEA-PMHS-R706 undergoes a 2.6 wt % increase in mass after 300 min at 90% relative humidity, whereas the increase for the paint film consisting of unmodified R706 pigment is 3.1 wt %. This represents a 19.2% increase in water uptake in the paint film formulated with R706 relative to that formulated with TEA-PMHS-R706. Such a decreased water uptake in a paint film formulated with hydrophobically modified R706 pigment is similar to the 21.9% lower water uptake previously observed upon similar 90% relative humidity treatment for a paint film consisting of hydrophobically modified TMS-capped R706 pigment, relative to the one with unmodified R706.[13]

The lower water uptake in the TEA-PMHS-R706 paint film is consistent with better association between the binder and pigment in the final paint film, when the pigment surface is hydrophobically modified with grafted PMHS, rather than that with unmodified R706 pigment surface, which has a contact angle considerably smaller than 90°. Although DVS data demonstrate a similar decrease in water uptake for TEA-PMHS-R706 and previously reported TMS-R706 pigment,[13] for both the dry powder and when formulated in a paint film relative to unmodified R706, the distinct advantage of TEA-PMHS-R706 is its ability to disperse as a low viscosity liquid in an aqueous slurry at high solids fractions (in particular above 70 wt % (37 vol %)), with the additional benefit of being able to do so with no added dispersant. Dispersion at these high mass loadings is a crucial attribute for commercial paint pigments. Being able to achieve this in water for a pigment particle that is highly hydrophobic upon drying is an unusual feat—even more so when considered that this dispersion occurs without any added dispersant. In comparison, these high solids fractions lead to a paste rather than a liquid dispersion, even with added dispersants, for previously reported TMS-R706, and even for native hydrophilic (unmodified) R706 at 75 wt % (43 vol %).

CONCLUSIONS

We demonstrate hydrophobic surface modification of hydrophilic native oxide surfaces of various pigments, which results in stable liquid dispersions in water at concentrations of up to 75 wt % (43 vol %). All unmodified pigments without dispersant are unable to form liquid dispersions at such high solids concentrations. In the absence of added dispersant, we attribute some of the observed dispersion stability of the hydrophobically modified pigments to steric stabilization resulting from the grafted PMHS strands on the R706 surface. Combining PMHS-R706 with low levels of a nonionic surfactant enables particle dispersion with no aggregation and similar rheology to benchmark optimal dispersions of the native oxide pigment, which rely on commercial polyanion dispersants. A combination of TGA and ^{29}Si CP/MAS NMR spectroscopy shows that TEA-PMHS-R706 particles preserve a less condensed, more loosely bound grafted PMHS fraction on the modified pigment surface, in addition to a more rigidly grafted PMHS layer. The more rigidly grafted PMHS is attributed to the first monolayer, while the loosely bound fraction in TEA-PMHS-R706 is thought to involve a multilayer via grafting to the monolayer. When using a different amine catalyst for PMHS grafting, AMP-PMHS-R706, only a rigid grafted PMHS layer is obtained. This more loosely bound fraction of TEA-PMHS-R706 contributes to the greater steric stabilization and lower viscosities of dispersions relative to AMP-PMHS-R706. Consistent with our previous results dealing with aqueous dispersions of hydrophobically modified pigment particles, using alkylsilane capping agents, which established that these surface-modified pigments lead to improved hydrophilic stain resistance, reduced water uptake, and tighter association with hydrophobic polymer in the dry state, paints formulated with the current hydrophobically modified PMHS-R706 pigments display improved water-barrier properties similar to those modified previously with alkylsilanes.

ASSOCIATED CONTENT

Supporting Information

The Supporting Information is available free of charge on the ACS Publications website at DOI: 10.1021/acs.langmuir.8b01898.

Synthesis and characterization data of surface-modified pigment particles (PDF)

AUTHOR INFORMATION

Corresponding Authors

*E-mail: kbeshah@dow.com (K.B.).
*E-mail: askatz@berkeley.edu (A.K.).

ORCID

Manish K. Mishra: 0000-0002-2901-628X
Ahmet Kusoglu: 0000-0002-2761-1050
Adam Z. Weber: 0000-0002-7749-1624
Alexander Katz: 0000-0003-3487-7049

Notes

The authors declare no competing financial interest.

ACKNOWLEDGMENTS

This work was funded by The Dow Chemical Company.

REFERENCES

(1) Braun, J. H.; Baidins, A.; Marganski, R. E. TiO_2 pigment technology: a review. *Prog. Org. Coat.* **1992**, *20*, 105−138.
(2) Farrokhpay, S. A review of polymeric dispersant stabilisation of titania pigment. *Adv. Colloid Interface Sci.* **2009**, *151*, 24−32.
(3) Thomas, N. L. The barrier properties of paint coatings. *Prog. Org. Coat.* **1991**, *19*, 101−121.
(4) Huldén, M.; Hansen, C. M. Water Permeation in Coatings. *Prog. Org. Coat.* **1985**, *13*, 171−194.
(5) Stieg, F. B., Jr. The Effect of Extenders on the Hiding Power of Titanium Pigments. *Off. Dig., Fed. Paint Varn. Prod. Clubs* **1959**, *31*, 52−64.
(6) Ingham, B.; Dickie, S.; Nanjo, H.; Toney, M. F. In situ USAXS measurements of titania colloidal paint films during the drying process. *J. Colloid Interface Sci.* **2009**, *336*, 612−615.
(7) Tiarks, F.; Frechen, T.; Kirsch, S.; Leuninger, J.; Melan, M.; Pfau, A.; Richter, F.; Schuler, B.; Zhao, C. L. Effects on the Pigment Distribution in Paint Formulation. *Macromol. Symp.* **2002**, *187*, 739−751.
(8) Landfester, K. Miniemulsion polymerization and the structure of polymer and hybrid nanoparticles. *Angew. Chem., Int. Ed.* **2009**, *48*, 4488−4507.
(9) Kawaguchi, M.; Yamamoto, T.; Kato, T. Rheological Studies of Hydrophilic and Hydrophobic Silica Suspensions in the Presence of Adsorbed Poly(N-isopropylacrylamide). *Langmuir* **1996**, *12*, 6184−6187.
(10) Trapani, A.; Bleuzen, M.; Kheradmand, J.; Koller, A.; Zukowski, L. The use of TiO_2-polymer composites to lower the environmental

DOI: 10.1021/acs.langmuir.8b01898
Langmuir 2018, 34, 11738−11748

impact and improve performance of waterborne paints. *Farby i Lakiery* **2013**, *5*, 8−18.
(11) Jankolovits, J.; Gazit, O. M.; Nigra, M. M.; Bohling, J.; Roper, J. A.; Katz, A. Single-Pot Encapsulation of Oxide Particles within a Polysaccharide Multilayer Nanocoating. *Adv. Mater. Interfaces* **2015**, *2*, No. 1400465.
(12) Poncet-Legrand, C.; Lafuma, F.; Audebert, R. Rheological Behaviour of Colloidal Dispersions of Hydrophobic Particles Stabilised in Water by Amphiphilic Polyelectrolytes. *Colloids Surf., A* **1999**, *152*, 251−261.
(13) (a) Jankolovits, J.; Kusoglu, A.; Weber, A. Z.; Van Dyk, A.; Bohling, J.; Roper, J. A.; Radke, C. J.; Katz, A. Stable Aqueous Dispersions of Hydrophobically Modified Titanium Dioxide Pigments through Polyanion Adsorption: Synthesis, Characterization, and Application in Coatings. *Langmuir* **2016**, *32*, 1929−1938. (b) Jankolovits, J.; Katz, A.; Bohling, J. C.; Radke, C. J.; Van Dyk, A. K.; Roper, J. A., III Aqueous Dispersion of Hydrophobically Modified Pigment Particles. U.S. Patent 9,957,403, 2018.
(14) Davies, R.; Schurr, G. A.; Meenan, P.; Nelson, R. D.; Bergna, H. E.; Brevett, C. A. S.; Goldbaum, R. H. Engineered Particle Surfaces. *Adv. Mater.* **1998**, *10*, 1264−1270.
(15) Genovese, D. B. Shear rheology of hard-sphere, dispersed, and aggregated suspensions, and filler-matrix composites. *Adv. Colloid Interface Sci.* **2012**, *171*−*172*, 1−16.
(16) *Chemours Technical Data Sheet*. https://chemours.com/Titanium_Technologies/en_US/assets/downloads/Ti-Pure-R-706-product-information.pdf.
(17) Lin, J.; Chen, H.; Yuan, Y.; Ji, Y. Mechanochemically conjugated PMHS/nano-SiO_2 hybrid and subsequent optimum grafting density study. *Appl. Surf. Science* **2011**, *257*, 9024−9032.
(18) Greco, P. P.; Stedile, F. C.; Dos Santos, J. H. Z. Influence of PMHS loading on the silica surface, on catalyst activity and on properties of resulting polymers. *J. Mol. Catal. A: Chem.* **2003**, *197*, 233−243.
(19) Nagappan, S.; Ha, C.-S. Effect of Sodium Hydroxide on the Fast Synthesis of Superhydrophobic Powder from Polymethylhydrosiloxane. *J. Coat. Sci. Technol.* **2014**, *1*, 151−160.
(20) Siebold, A.; Walliser, A.; Nardin, M.; Oppliger, M.; Schultz, J. Capillary Rise for Thermodynamic Characterization of Solid Particle Surface. *J. Colloid Interface Sci.* **1997**, *186*, 60−70.
(21) Yilbas, B. S.; Hassan, G.; Al-Shara, A.; Ali, H.; Al-Aqeeli, N.; Al-Sarkhi, A. Water Droplet Dynamics on a Hydrophobic Surface in Relation to the Self-Cleaning of Environmental Dust. *Sci. Rep.* **2018**, *8*, No. 2984.
(22) (a) Chatterjee, T.; Nakatani, A. I.; Van Dyk, A. Shear-Dependent Interactions in Hydrophobically Modified Ethylene Oxide Urethane (HEUR) Based Rheology Modifier−Latex Suspensions: Part 1. Molecular Microstructure. *Macromolecules* **2014**, *47*, 1155−1174. (b) Van Dyk, A.; Nakatani, A. Shear rate-dependent structure of polymer-stabilized TiO_2 dispersions. *J. Coat. Technol. Res.* **2013**, *10*, 297−303.
(23) Deák, A.; Hild, E.; Kovács, A. L.; Hórvölygi. Contact angle determination of nanoparticles: film balance and scanning angle reflectometry studies. *Phys. Chem. Chem. Phys.* **2007**, *9*, 6359−6370.
(24) Sakai, N.; Wang, R.; Fujishima, A.; Watanabe, T.; Hashimoto, K. Effect of Ultrasonic Treatment on Highly Hydrophilic TiO_2 Surfaces. *Langmuir* **1998**, *14*, 5918−5920.
(25) Moitra, N.; Ichii, S.; Kamei, T.; Kanamori, K.; Zhu, Y.; Takeda, K.; Nakanishi, K.; Shimada, T. Surface functionalization of silica by Si-H activation of hydrosilanes. *J. Am. Chem. Soc.* **2014**, *136*, 11570.
(26) Yang, D.; Xu, Y.; Xu, W.; Wu, D.; Sun, Y.; Zhu, H. Tuning pore size and hydrophobicity of macroporous hybrid silica films with high optical transmittance by a non-template route. *J. Mater. Chem.* **2008**, *18*, 5557.
(27) Ma, C. D.; Wang, C.; Acevedo-Vélez, C.; Gellman, S. H.; Abbott, N. L. Modulation of Hydrophobic Interactions by Proximally Immobilized Ions. *Nature* **2015**, *517*, 347−350.
(28) Mewis, J.; Wagner, N. J. *Colloidal Suspension Rheology*, 1st ed.; Cambridge University Press: Cambridge, 2012.
(29) Stathatos, E.; Lianos, P.; Del Monte, F.; Levy, D.; Tsiourvas, D. Formation of TiO_2 Nanoparticles in Reverse Micelles and Their Deposition as Thin Films on Glass Substrates. *Langmuir* **1997**, *13*, 4295−4300.
(30) Burnside, S. D.; Shklover, V.; Barbé, C.; Comte, P.; Arendse, F.; Brooks, K.; Grätzel, M. Self-Organization of TiO_2 Nanoparticles in Thin Films. *Chem. Mater.* **1998**, *10*, 2419−2425.
(31) Chhabra, V.; Pillai, V.; Mishra, B. K.; Morrone, A.; Shah, D. Synthesis, characterization and properties of microemulsion-mediated nanophase TiO_2 particles. *Langmuir* **1995**, *11*, 3307−3311.
(32) Carretti, E.; Giorgi, R.; Berti, D.; Baglioni, P. Oil-in-water nanocontainers as low environmental impact cleaning tools for works of art: Two case studies. *Langmuir* **2007**, *23*, 6396−6403.
(33) Farrokhpay, S. A review of polymeric dispersant stabilisation of titania pigment. *Adv. Colloid Interface Sci.* **2009**, *151*, 24−32.
(34) Mari, R.; Seto, R.; Morris, J. F.; Denn, M. M. Discontinuous shear thickening in Brownian suspensions by dynamic simulation. *Proc. Natl. Acad. Sci. U.S.A.* **2015**, *112*, 15326−15330.
(35) Delacy, B.; Redding, D. R.; Matthews, J. *Optical, Physical, and Chemical Properties of Surface Modified Titanium Dioxide Powders*, ECBC-TR-835; Science Applications International Corporation: Gunpowder, MD, 2011.
(36) Katz, A.; Davis, M. Molecular Imprinting of Bulk, Microporous Silica. *Nature* **2000**, *403*, 286.
(37) Bauer, F.; Decker, U.; Dierdorf, A.; Ernst, H.; Heller, R.; Liebe, H.; Mehnert, R. Preparation of moisture curable polysilazane coatings: Part I. Elucidation of low temperature curing kinetics by FT-IR spectroscopy. *Prog. Org. Coat.* **2005**, *53*, 183−190.
(38) Gao, X.; Zhou, B.; Guo, Y.; Zhu, Y.; Chen, X.; Zheng, Y.; Gao, W.; Ma, X.; Wang, Z. Synthesis and characterization of well-dispersed polyurethane/$CaCO_3$ nanocomposites. *Colloids Surf., A* **2010**, *371*, 1−7.
(39) Caravajal, G. S.; Leyden, D. E.; Quinting, G. R.; Maciel, G. E. Structural characterization of (3-aminopropyl)triethoxysilane-modified silicas by silicon-29 and carbon-13 nuclear magnetic resonance. *Anal. Chem.* **1988**, *60*, 1776−1786.
(40) Yang, D.; Xu, Y.; Xu, W.; Wu, D.; Sun, Y.; Zhu, H. Tuning pore size and hydrophobicity of macroporous hybrid silica films with high optical transmittance by a non-template route. *J. Mater. Chem.* **2008**, *18*, 5557−5562.
(41) Litvinov, V. M.; Barthel, H.; Wets, J. Structure of a PDMS Layer Grafted onto a Silica Surface Studied by Means of DSC and Solid-State NMR. *Macromolecules* **2002**, *35*, 4356−4364.
(42) Pines, A.; Gibby, M. G.; Waugh, J. S. Proton-enhanced NMR of Dilute Spins in Solids. *J. Chem. Phys.* **1973**, *59*, 569−590.
(43) Napper, D. A. *Polymeric Stabilization of Colloidal Dispersions*; Academic Press, 1984.
(44) Napper, D. H.; Netschey, A. Studies of the Steric Stabilization of Colloidal Particles. *J. Colloid Interface Sci.* **1971**, *37*, 528−535.
(45) Zhulina, E. B.; Borisov, O. V.; Priamitsyn, V. A. Theory of Steric Stabilization of Colloid Dispersions by Grafted Polymers. *J. Colloid Interface Sci.* **1990**, *137*, 495−511.
(46) Nowicki, W. Structure and Entropy of a Long Polymer Chain in the Presence of Nanoparticles. *Macromolecules* **2002**, *35*, 1424−1436.

DOI: 10.1021/acs.langmuir.8b01898
Langmuir 2018, 34, 11738−11748